

Computed Microtomography and X-ray Fluorescence Analysis for Comprehensive Analysis of Structural Changes in Bone

Alexey Buzmakov, Marina Chukalina, Dmitry Nikolaev, Gerald Schaefer, Victoria Gulimova,
Sergey Saveliev, Elena Tereschenko, Alexey Seregin, Roman Senin, Victor Prun,
Denis Zolotov and Victor Asadchikov

Abstract—This paper presents the results of a comprehensive analysis of structural changes in the caudal vertebrae of Turner’s thick-toed geckos by computer microtomography and X-ray fluorescence analysis. We present algorithms used for the reconstruction of tomographic images which allow to work with high noise level projections that represent typical conditions dictated by the nature of the samples. Reptiles, due to their ruggedness, small size, belonging to the amniote and a number of other valuable features, are an attractive model object for long-orbital experiments on unmanned spacecraft. Issues of possible changes in their bone tissue under the influence of spaceflight are the subject of discussions between biologists from different laboratories around the world.

I. INTRODUCTION

Terrestrial organisms exposed to microgravity during spaceflight experience musculoskeletal structure changes. Reptiles, due to their ruggedness, small size, belonging to the amniote and a number of other valuable features, are an attractive model object for long-orbital experiments on unmanned spacecraft [1], [2]. By adhesion, Turner’s thick-toed geckos remain in weightlessness as a response of support and locomotion. The gecko’s tail is not prehensile, and is rarely used for support during locomotion. Rather, it plays the role of the rocker, communication and storage of fat reserves. Therefore, its experienced mechanical loads can be considered negligible. With this in mind, the caudal vertebrae are chosen as the object of study. Geckos of the mission groups and delayed synchronous control groups were investigated.

In this paper, we present the results of a comprehensive analysis of structural changes in the caudal vertebrae of Turner’s thick-toed geckos by X-Ray fluorescence analysis (XRFA) and computed microtomography (CT). X-ray fluorescence measurements for qualitative analysis of the sam-

ples were performed with an X-ray diffractometer Rigaku SmartLab. A thermoelectrically cooled passivated implanted planar silicon detector was used for recording the spectra. Computed tomography with monochromatic X-ray beams was performed at the Shubnikov Institute of Crystallography, RAS [3] and at beamlines RT-MT and MEDIANA at the Kurchatov Center for Synchrotron Radiation and Nanotechnology. Three energy values (5.4, 8.0 and 12.0 keV) were chosen in order to achieve greater sensitivity to different absorbers. The use of CT reconstruction algorithms presented in this paper allows to work with high noise level projections that represent typical conditions dictated by the nature of the samples.

II. REGULARISED ALGEBRAIC RECONSTRUCTION TECHNIQUE

In our CT experiments, the parallel scanning scheme, as depicted in Figure 1 has been used. Wide monochromatic parallel X-ray beams cross the sample boundary and only part of the photons emerge from the other side of the sample. These photons are unaffected by either absorption or scatter and therefore propagate in their original direction of travel. A position-sensitive detector registers the photons (tomographic projections). Then the sample is rotated by the angle of projection j , and the procedure is repeated. The Radon transform can be used to compute projections of an image matrix (distribution of linear attenuation coefficients) along specified directions. The problem is to reconstruct the image matrix f from the set of projections p . The main approaches employed for this are transform-based and algebraic reconstruction techniques (CT algorithms). Although conceptually the algebraic approach is much simpler compared to transform-based methods, it is also rather slow due to its computational complexity. Recent progress in computer chip design and production, specifically GPU (graphical processing unit)-based parallel computing architectures such as those developed by nVIDIA, however enable a reasonable running time as we discuss in this paper.

For the algebraic approach [4], a square grid is imposed on the image. As the function f is constant in each pixel, we will search the solution in the space of piecewise constant functions. X-rays are lines running through the image plane, and we assume that the ray width is approximately equal to the pixel size. The relation between p , the ray sum, and f is

A. Buzmakov, V. Asadchikov, E. Tereschenko, A. Seregin and D. Zolotov are with the Shubnikov Institute of Crystallography RAS, Moscow, Russia.

M. Chukalina is with the Institute of Microelectronics Technology and High Purity Materials RAS, Chernogolovka, Russia.

D. Nikolaev is with the Institute for Information Transmission Problems (Kharkevich Institute) RAS, Moscow, Russia.

G. Schaefer is with the Department of Computer Science, Loughborough University, Loughborough, U.K.

V. Gulimova and S. Saveliev are with the Research Institute of Human Morphology RAMS, Moscow, Russia.

R. Senin is with the Kurchatov Center for Synchrotron Radiation and Nanotechnology, Moscow, Russia.

V. Prun is with the Moscow Institute of Physics and Technology and with the Shubnikov Institute of Crystallography RAS, Moscow, Russia.

This work was partly supported by RFBR grant 11-02-12110-ofi-m.

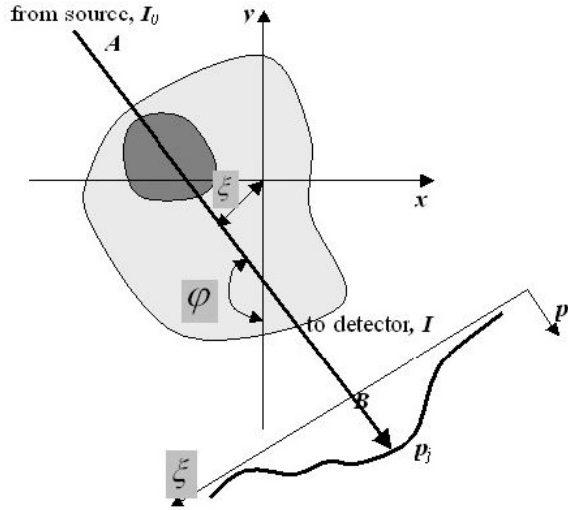


Fig. 1. Parallel scanning scheme.

expressed as

$$p_j = (f, w_j), j = 1, 2, \dots, M \quad (1)$$

where w_j is the weighting factor vector that represents the contribution of the pixels to the j -th ray sum, and M is the number of projection angles.

For large numbers of pixels and rotation angles there exist iterative methods to solve the equation system. These are based on the “method of projections” first proposed by Kaczmarz. An image f is considered to be a single point in an N -dimensional space. Each of the linear equations defines a hyperplane, and the unique solution to these equations is the intersection of all hyperplanes.

Let f^k be the estimated solution in the k -th iteration. The iteration scheme is then represented by

$$f^{k+1} = f^k + \gamma \frac{p_j - (f^k, w_j)}{(w_j, w_j)} w_j \quad (2)$$

where γ is the so-called relaxation parameter, and j is the rotation angle.

It was shown [5] that the limits of cyclic sub-sequences generated by the method reduce to a weighted least squares solution of the system when the relaxation parameter approaches zero. This point minimises the sum of squares of Euclidean distances to the hyperplanes of the system.

The initial estimate is projected onto the hyperplane represented by the first equation in Eq. (2). After each projection to a hyperplane, the estimated image f is updated. The first sub-iteration is finished once the correction over all hyperplanes has been performed.

Many projection access schemes have been discussed in the literature [6]. To minimise the influence of two neighbouring hyperplanes on each other we used the scheme mentioned in [7]. Because the projections are usually noisy, the intersection of the hyperplanes is not a point in the N -dimensional space but a polyhedron. Each iteration projects

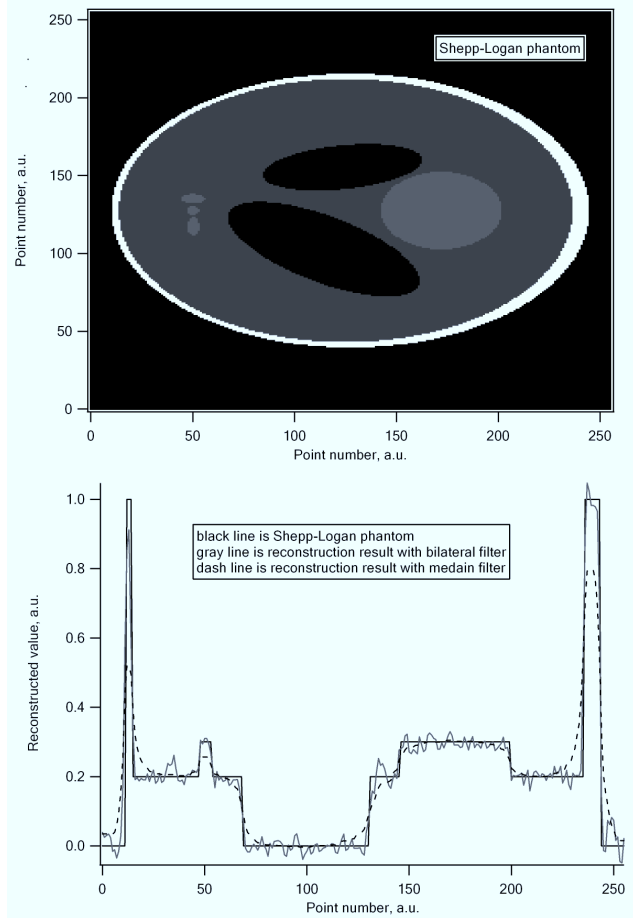


Fig. 2. Shepp-Logan phantom (top) and cross-section of the reconstructed phantom based on reconstruction employing median and bilateral filters (bottom). 180 projection angles were taken to simulate the sinogram.

the estimated solution to a polyhedron hull area. A regularisation operator brings the estimated solution from the polygon wall area to the image sub-space. We have taken the space of piecewise smooth functions as the image space, and evaluated median and bilateral filters as projectors from the polygon wall area to the image sub-space. A comparison between these two regularisation methods on a Shepp-Logan phantom is shown in Fig. 2. In following experiments, we then employed the simpler median filter for regularisation.

One iteration is completed once the full set of measurements has been processed. In the next iteration, f^k is projected onto the hyperplane represented by the first equation in Eq. (2), and successively onto the rest of the hyperplanes. Then, filtering is applied and so on until the last iteration. In the last iteration, all images are saved. The final step of the algorithm is the averaging over these images to exclude the influence of the last hyperplane projection.

We employ a rotation technique involving 2D texture fetching using CUDA technology to reduce memory bandwidth. CUDA¹ (as well as ATI Stream and similar technologies) allow a large part of computationally intensive calcula-

¹http://www.nvidia.com/object/cuda_home.html

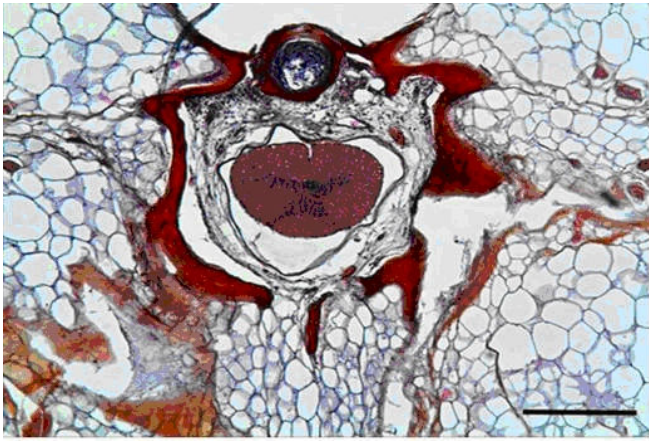


Fig. 3. Example, stained with hematoxylin-eosin at 5x magnification. The length scale feature length is 300 microns.

tions to be propagated to an array of graphical processor units (GPUs). The bilinear rotation algorithm includes two almost independent stages for each pixel of the destination image: calculation of its exact co-ordinates on the source image, and bilinear interpolation of the value around this point. The used CUDA texture fetching mechanism allows implementation of the second stage on hardware level completely transparent for the programmer.

III. SAMPLE DESCRIPTION

Bones of proximal caudal vertebrae of geckos (*Chondrodactylus turneri* Gray, 1864) were studied; Figure 3 shows an example. Geckos live in Central and Southern Africa, inhabiting a variety of habitats from rocky deserts to humid coastal rivers. The total body length from tip of nose to tip of tail is about 13-15 cm. These reptiles have been proposed [2] and successfully used as a model object for studying the amniote for unmanned spacecraft FOTON-2 and FOTON-3.

By adhesion, geckos remain in weightlessness as a response of support and locomotion. The gecko's tail is not prehensile, and is rarely used for support during locomotion but mainly plays the role of the rocker, communication and storage of fat reserves. Therefore, its experienced mechanical loads can be considered negligible. For biologists it is important to answer the question of possible changes in the bone under the influence of space flight.

Geckos of the mission groups (F) and delayed synchronous control groups (S) were investigated in this study.

IV. RESULTS

X-ray fluorescence measurements for qualitative analysis of the samples were performed with an X-ray diffractometer Rigaku SmartLab with rotating anode using Mo K_{α} radiation at the Shubnikov Institute of Crystallography, RAS. Monochromatisation and collimation of the radiation were provided with a focussing mirror and a diffractive double monochromator Ge (220). Samples were placed on a polished silicon wafer with a known chemical composition. An

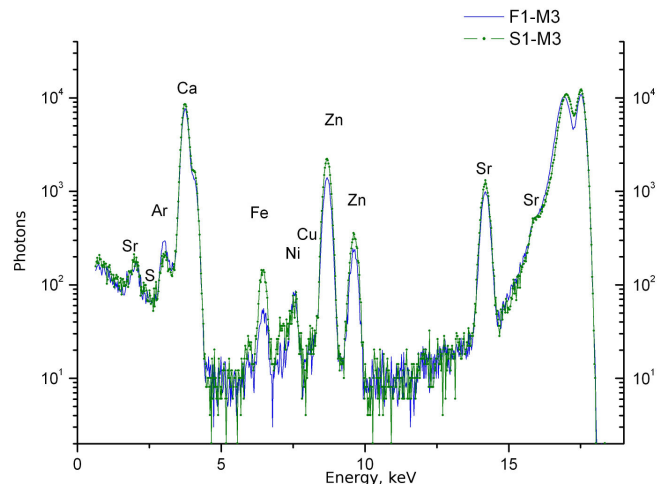


Fig. 4. Fluorescence spectra of samples S1-M3 and F1-M3 (Mission 3).

example of the measured spectra is shown in Fig. 4. The spectra were processed using the PyMca software².

The results of the analysis were used to establish the elemental composition of samples required to select the correct conditions for the realisation of CT experiments as well as to identify possible differences in samples of M2 and M3 groups.

Computed tomography with monochromatic X-ray beams was performed at the Shubnikov Institute of Crystallography, RAS [3] and at beamlines RT-MT and MEDIANA at the Kurchatov Center for Synchrotron Radiation and Nanotechnology. The three energy values (5.4, 8.0 and 12.0 keV) were chosen in order to achieve greater sensitivity to different absorbers. This allows to determine the location of chemical elements with jumps of the absorption coefficient of X-ray radiation. An example of a reconstructed CT image is shown in Figure 5.

Studies have shown that the peripheral areas of the samples did not contain elements with atomic number 20 (Ca) (or that their concentration is below the sensitivity of the method). Identified areas of higher density are close to the centre channel. Uneven distribution of heavy elements are detected. Correlation was found between the CT data and the results of XRFA.

V. CONCLUSIONS

In this paper we have reported on an analysis of structural changes in the caudal vertebrae of geckos by XRFA and computed microtomography, and presented CT reconstruction algorithms which allow working also with very noisy projections. Preliminary histological examination showed that the studied samples are very heterogeneous. Some of these differences could affect the results of CT and XRFA, for example differences in the methods of fixation of the samples, individual differences in animals etc. In future work, we plan to continue our calculations to organise, summarise and interpret the gained information.

²<http://pymca.sourceforge.net/>

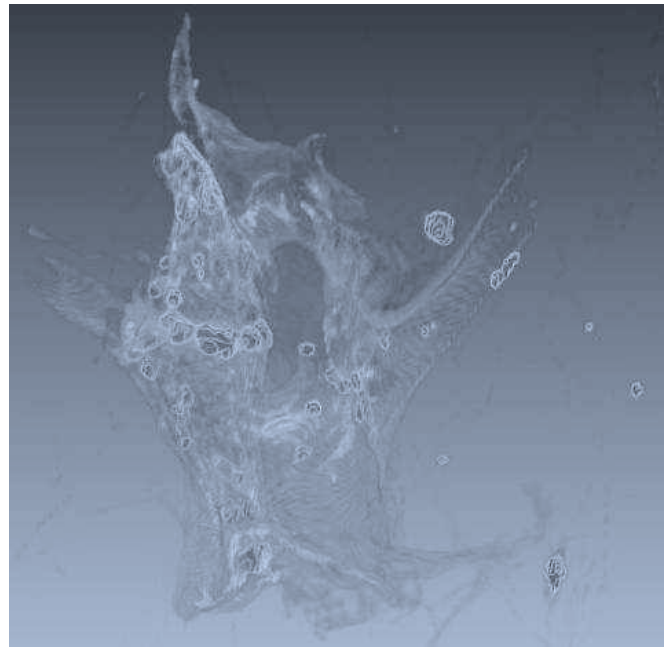
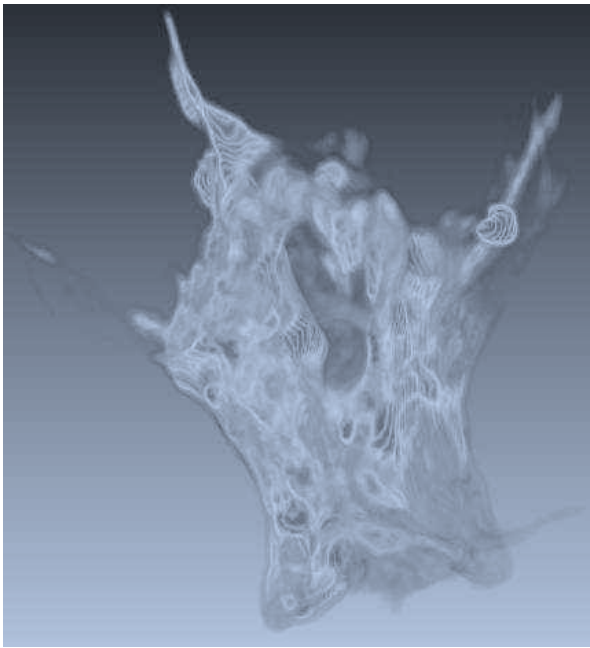


Fig. 5. Reconstructed CT image of F1-M3 sample with beam energies of 5.4 keV (left) and 13 keV (right).

REFERENCES

- [1] E. Almeida, C. Roden, J. Phillips, R. Yusuf, R. Globus, N. Searby, W. Vercootere, E. Morey-Holton, V. Gulimova, S. Saveliev, M. Tairbekov, U. Iwaniec, A. McNamra, and R. Turner, "Development of the gecko (*pachydactylus turnery*) animal model during foton m-2 to study comparative effects of microgravity in terrestrial and aquatic organisms." *Journal of Gravitational Physiology*, vol. 13, no. 1, pp. 193–196, 2006.
- [2] V. Gulimova, V. Nikitin, V. Asadchikov, A. Buzmakov, I. Okshtein, E. Almeida, E. Ilyin, and S. Tairbekov, M.G.and Saveliev, "Effect of 16-day spaceflight on the morphology of thick-toed geckos (*pachydactylus turnery* gray, 1846)." *Journal of Gravitational Physiology*, vol. 13, no. 1, pp. 197–200, 2006.
- [3] V. Asadchikov, A. Buzmakov, D. Zolotov, R. Senin, and A. Geranin, "Laboratory x-ray microtomographs with the use of monochromatic radiation." *Crystallography Reports*, vol. 55, no. 1, pp. 158–167, 2010.
- [4] R. A. Gordon, "A tutorial on ART (algebraic reconstruction technique)," *IEEE Trans. Nuclear Science*, vol. 21, pp. 78–93, 1974.
- [5] Y. Censor, P. Eggermont, and D. Gordon, "Strong underrelaxation in Kaczmarz's method for inconsistent systems," *Numerische Mathematik*, vol. 41, no. 1, pp. 83–92, 1983.
- [6] H. Guan and R. Gordon, "Computed tomography using algebraic reconstruction techniques (ARTs) with different projection access schemes: A comparison study under practical situations," *Phys. Med. Biol.*, vol. 41, pp. 1727–1743, 1996.
- [7] A. Buzmakov, D. Nikolaev, M. Chukalina, and G. Schaefer, "Efficient and effective regularised ART for computed tomography," in *Annual Int. Conference of the IEEE EMBS*, 2011, pp. 6200–6203.